A Whole-Body 7 Tesla RF Excitation Scheme with Much Improved B1+ Field Homogeneity and Local/Global SARs over Quadrature Excitation

T. S. Ibrahim[1,2] and L. Tang[3]

[1]University of Pittsburgh, Pittsburgh, Pennsylvania, United States, [2]University of Oklahoma, Norman, Oklahoma, United States, [3]Electrical & Computer Engineering, University of Oklahoma, Norman, OK, United States

Introduction: MRI at higher field strengths corresponds to increased operational frequencies (*1, 2*). At these frequencies, the wavelengths of the electromagnetic waves produced by currents on RF coils/transmit arrays become on the order of fractions of the human body size. At such conditions, the electromagnetic waves interact with the human body in a complex/non-intuitive manner requiring the use of full wave electromagnetic models for interpretation purposes. Additionally, at such field strength and anatomical loads, the electric and magnetic fields become highly coupled. As such, the relationship between the distribution/intensity of circularly polarized component of the transverse magnetic (B_1^+) field and the total RF power absorption as well as the specific absorption rate (SAR) become extremely complex, typically resulting in high power deposition and higher peak SARs. In this work, with the assistance of the finite difference time domain (FDTD), we demonstrate that compared to the standard 2-/4-/n- port quadrature excitations, 7 Tesla whole-body phased-array RF excitation (without the use of transmit SENSE) can simultaneously 1) significantly improve the B_1^+ field homogeneity across 2-D and large 3-D regions of the human body, 2) lower the total absorbing power in the whole-body, and 3) lower the peak SARs.

Methods: An FDTD mesh of a 32-strut coupled-element TEM coil was numerically designed at 7 Tesla. After loading the coil with an anatomically accurate human body model, the coil was tuned to the desired 7 Tesla operation (approximately 295 MHz). The B_1^+ field, the total power absorbed in the whole body including the portions outside the coil cavity, and SARs were considered as three optimization parameters as calculated from Equations (1-3), respectively:

$$B_1^+ = \left|\frac{B_{1x} + j * B_{1y}}{\sqrt{2}}\right|; (1) \qquad Power = \sum_i \sum_j \sum_k [\frac{1}{2}\sigma_{(i,j,k)} \times (E^2_{x_{(i,j,k)}} + E^2_{y_{(i,j,k)}} + E^2_{z_{(i,j,k)}})]; (2) \qquad SAR_{(i,j,k)} = \frac{1}{2}\frac{\sigma_{(i,j,k)}(E^2_{x_{(i,j,k)}} + E^2_{y_{(i,j,k)}} + E^2_{z_{(i,j,k)}})}{\rho_{(i,j,k)}} (3).$$

In equations (1-3), B_{1x} and B_{1y} are the *x* and *y* components of the B_1 field; $\sigma_{(i,j,k)}$ (S/m) is the conductivity of the FDTD cell at the *(i,j,k)* location; E_x, E_y and E_z (V/m) are the amplitudes of the electric field components in the *x*, *y*, and *z* directions, respectively, and $\rho_{(i,j,k)}$ is the tissue density at location *(i,j,k)*. Based on the coil in question and on variable phase/variable amplitude phased-array excitation, an optimization routine that combines genetic and gradient algorithms was implemented to improve the homogeneity of the B_1^+ field as denoted by the coefficient of variation (COV) across 3-D slabs and organs, while reducing 1) the total power absorbed by the whole body, and 2) the local SARs. All the power and SAR calculations were scaled to obtain 1.96 (μT) B_1^+ field, which is the field strength needed to produce a flip angle of π/2 with a 3-msec rectangular RF pulse.

Results and Conclusions: Using the gradient/genetic based optimization algorithm, 5 slices (6-mm thick and oriented in different directions), 5 slabs (84-mm thick and oriented in different directions), and 3-D regions (heart and pancreas) were optimized pursuing more homogeneous B_1^+ field distribution, lower total power absorbed by the whole-body, and lower peak SARs to avoid "hot spots". Similar to fluid-dynamics Mach number (*3*), the optimization target/goal combines all of these three parameters into a non-linear relationship and was constantly changing throughout the iterations. Figure 1 and Table 1 show some samples of the results including the B_1^+ field distributions, the associated RF power deposition, and peak SARs before (using 32-port quadrature excitation) and after (variable phases/amplitude) optimization. Due to the difference in the SAR FDA regulations on extremities and non-extremities, the optimizations were considered with and without the arms (note that the arms were always present in the coil and were not removed from the field calculations). The results demonstrate that B_1^+ field uniformity can be greatly improved (on the order of 3-5 times) while significantly reducing 1) the total power deposition and 2) imbalanced (local SAR) heating. Such results indicate that the original (quadrature) severe inhomogeneity is resultant from the lack of B_1^+ field but not necessarily from the lack of electromagnetic energy.

The positions of the peak SARs are shown in Figure 2. When including the arms, Figure 2 illustrates that the locations of peak SARs before and after slab optimization are all in the arms. When examining the peak SARs in the abdomen with both arms removed, the B_1^+ field uniformity could be increased to about the same level as in the case where the arms are included, yet significant reduction in the total power absorption and peak SARs could be achieved as well.

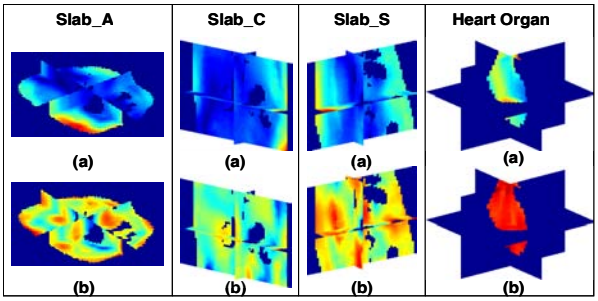

Figure 1: The B_1^+ field distributions at 7 Tesla before (quadrature) (a) and after (b) 3-D optimizations on Slab_A, slab_C, Slab_S, and the heart organ. All three slabs are 84mm thick. Slab_ A is an axial slab located at the center of the coil; Slab_C and Slab_S are 252mm long in coronal and sagittal directions, respectively.

Figure 2: Positions of the peak SARs before (quadrature) (Δ) and after (o) optimization over 5 84-mm slabs (3axial/1 coronal/1sagittal) with (left) and without (right) the arms included in the optimizations.

Optimizations			COV	Abs. Power (w)	Peak SAR (w/kg)
Slab_A	Qua	w/a	0.65	687.2	115.1
		wo/a	0.65	355.5	21.0
	Opt	w/a	0.23	330.5	46.0
		wo/a	0.22	230.5	11.2
Slab_C	Qua	w/a	0.63	2080.3	348.5
		wo/a	0.63	1082.9	64.0
	Opt	w/a	0.22	850.5	89.8
		wo/a	0.22	590.4	42.8
Slab_S	Qua	w/a	0.53	1040.4	174.3
		wo/a	0.53	541.61	32.0
	Opt	w/a	0.20	688.0	76.8
		wo/a	0.22	333.9	15.4
Heart Organ	Qua	w/a	0.31	1832.4	307.0
		wo/a	0.31	953.9	56.3
	Opt	w/a	0.06	1710.5	232.38
		wo/a	0.11	679.0	51.0

Table 1: Coefficient of variation (COV), absorbed power, and peak SARs using quadrature (Qua) and optimized (Opt) excitations with (w/a) and without the arms (wo/a) included as a port of the power deposition.

1. T. Vaughan *et al.*, the Proceedings 14th Scientific Meeting, International Society for Magnetic Resonance in Medicine, Seattle, May 2006.
2. L. Wald *et al.*, the Proceedings 14th Scientific Meeting, International Society for Magnetic Resonance in Medicine, Seattle, May 2006.
3. J. H. Zhao, J. O. Burns, M. L. Norman, M. E. Sulkanen, *Astrophysical Journal* 387, 83 (Mar, 1992).